Ambient particulate matter, VOC, NO_2 and SO_2 in the vicinity of Antwerp International Airport during 2024

Greenpeace Research Laboratories Technical Report GRL-TR-01-2025, January 2025

Aidan Farrow[1]

[1]Greenpeace Research Laboratories, College of Life and Environmental Sciences, Innovation Centre Phase 2, University of Exeter, Exeter, United Kingdom.

Contents

Introduction

Antwerp International Airport is located within the city of Antwerp, approximately 4 km south-east of the city centre. Land adjacent to the airport contains residential areas, recreation and sports facilities, retail and industrial use. The nearby railway carries predominantly electric trains and is unlikely to be a significant air pollution source.

This report presents observations of fine particulate matter (PM_1, $PM_{2.5}$ and Total Particle Count), total volatile organic compounds (TVOC), nitrogen dioxide (NO_2), carbon monoxide (CO) and sulphur dioxide (SO_2) in ambient air made at a residential location close to the airport (Figure 1).

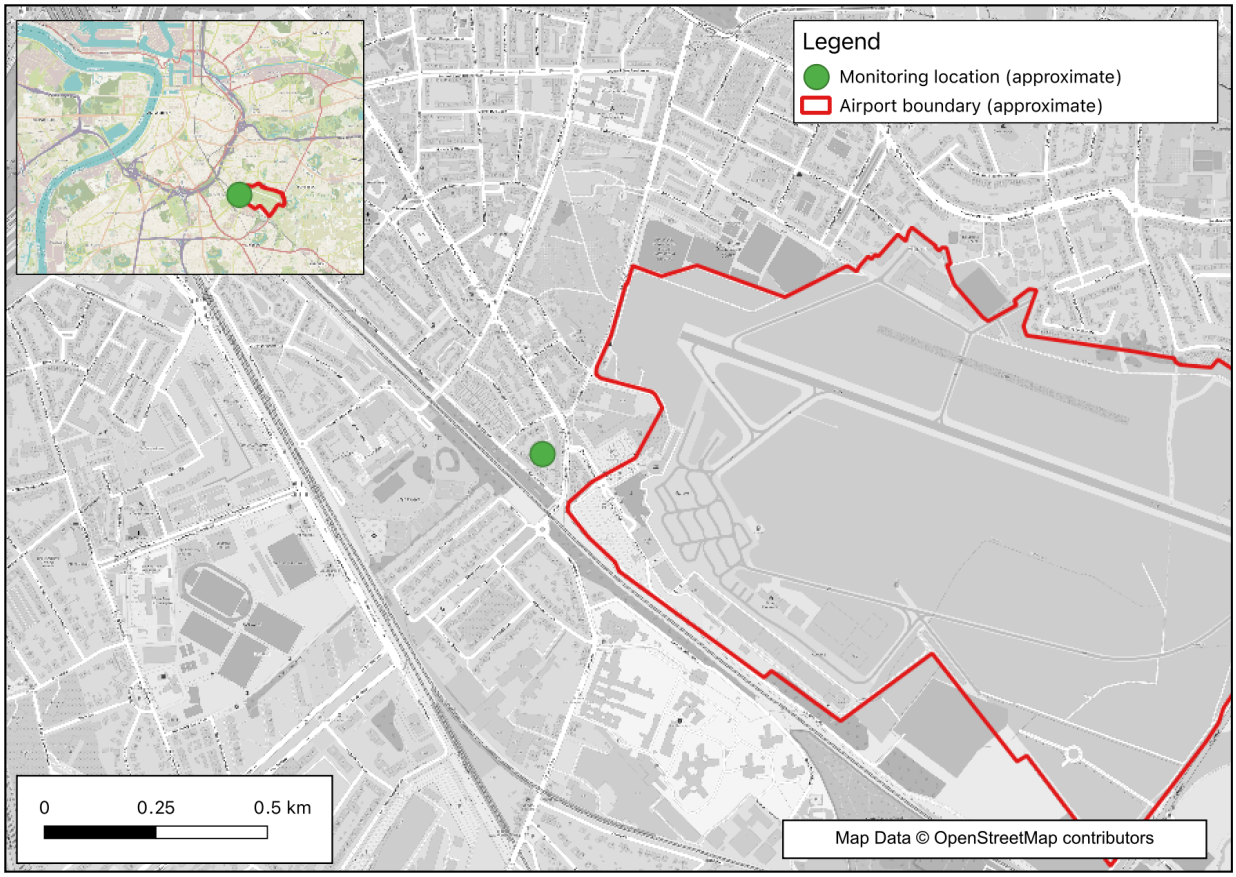

Figure 1. Antwerp airport and monitoring location[1,2]

Methods

Air quality observations were made using an AQMesh instrument. AQMesh pods (Environmental Instruments Ltd, UK, www.aqmesh.com) are self-contained units that measure ambient concentrations of gaseous and particulate air pollutants. Air quality data are gathered using electrochemical gas sensors, and an optical particle counter. They are processed by a proprietary algorithm which corrects for cross-interferences and for the effect of temperature and relative humidity. In the current study, the device was used to monitor concentrations of carbon monoxide (CO), nitrogen oxides (NO, NO_2), sulphur dioxide (SO_2), total volatile organic compounds (TVOC), particulate mass (PM_1, $PM_{2.5}$) and total particulate count (TPC), as well as a number of environmental variables (temperature, relative humidity and atmospheric pressure).

[1] OpenStreetMap data is open data, licensed under the Open Data Commons Open Database License (ODbL) by the OpenStreetMap Foundation (OSMF).
[2] OpenStreetMap contributors. (2015) Planet dump data file from August 2024. Retrieved from https://planet.openstreetmap.org

When using electrochemical gas sensors to estimate air pollutant concentrations, it is best practice to perform a field calibration to improve the accuracy of results and validate the measurements made. In preparation for the current study, the AQMesh instrument was co-located between 29th of March 2024 and 6th of May 2024 with the Antwerp Borgerhout monitoring station (42R801) by arrangement with the Flanders Environment Agency. A cross-comparison of the AQMesh and reference instrument was performed for PM_1, $PM_{2.5}$, NO and NO_2. Reference data were not available to perform a similar cross-comparison for CO, SO_2, TPC or TVOCs.

The relationship between observations made by the AQMesh and the reference monitor (Antwerp Borgerhout monitoring station) are shown in appendix figures A2 and A5. The cross-comparison was used to calculate scaling factors that could then be applied to the PM_1, $PM_{2.5}$, NO, and NO_2 data collected using the AQMesh. Details of this process are provided in Appendix 1. The AQMesh monitor differed from the reference monitor for NO (R^2=0.22) but was in good agreement for PM_1 (R^2=0.91) and $PM_{2.5}$ (R^2=0.89), and reasonable agreement for NO_2 (R^2=0.64). Therefore a correction factor was applied to the raw AQMesh PM_1, $PM_{2.5}$ and NO_2 data but NO data are not included in the analysis.

Data for CO, SO_2, TPC and TVOC are only treated with the AQMesh proprietary algorithm to correct for cross-interferences and for the effect of temperature and relative humidity.

After the PM_1, $PM_{2.5}$, NO and NO_2 cross-comparison, the AQMesh instrument was deployed at a residential location on Saffierstraat, Antwerp (west side of airport). Measurements of CO, NO_2, SO_2, TVOC, PM_1, $PM_{2.5}$, and TPC collected over the period from 16th of May to 21st November 2024 are presented and analysed below.

These air quality observations have been analysed in combination with meteorological data measured at Antwerp Airport and made available as part of the National Centres for Environmental Information (NCEI) Global Hourly Integrated Surface Database (ISD)[3].

All data were analysed using the Openair[4] and Worldmet[5] R software packages.

[3] NCEI (2024)Global Hourly Integrated Surface Database (ISD). https://www.ncei.noaa.gov/products/land-based-station/integrated-surface-database [Accessed 17/12/2024]

[4] Carslaw, D. C. and K. Ropkins, (2012) Openair --- an R package for air quality data analysis. Environmental Modelling & Software. Volume 27-28, 52-61.

[5] Carslaw D (2024). *worldmet: Import Surface Meteorological Data from NOAA Integrated Surface Database (ISD)*. R package version 0.9.7.9000, https://github.com/davidcarslaw/worldmet, https://davidcarslaw.github.io/worldmet/.

Results

Monitoring period statistics

Results from the monitoring period, between 16th of May to 21st November 2024 are presented in Table 1 and Figure 2. Monitoring period mean and daily maximum values are within current European Union standards[6] and World Health Organisation guidelines[7] for air quality over comparable averaging periods (Table 2). Minimum and maximum hourly concentrations indicate significant variability.

Table 1. Summary of hourly average air quality observations for the period 16 May - 21 November 2024.

Pollutant	Units	Mean	Min	Max	Median	Max daily	Rolling 8-hour max
CO	$\mu g/m^3$	253.0	46.8	1021.5	233.6	505.7	887.2
NO_2	$\mu g/m^3$	19.6	4.4	91.6	19.2	42.8	61.4
PM_1	$\mu g/m^3$	9.4	0.5	76.7	6.0	33.8	59.7
$PM_{2.5}$	$\mu g/m^3$	12.3	1.5	107.9	7.8	52.3	98.5
SO_2	$\mu g/m^3$	2.6	<5	172.7	0.0	37.0	88.2
TPC	$count/m^3$	5.6	0.3	44.9	3.5	21.6	36.0
TVOC	ppb	<10	<10	30.5	<10	<10	23.0

Table 2. Summary of relevant annual, daily and hourly average European Union air quality standards and World Health Organisation air quality guidelines.

Pollutant	Units	Averaging period	EU Standards (Current)[6]	EU Standards (2030)[8]	WHO Guidelines (2021)[7]
CO	$\mu g/m^3$	1 day	-	4,000	4,000
CO	$\mu g/m^3$	8 hour max	10,000	10,000	10,000
NO_2	$\mu g/m^3$	1 year	40	20	10

[6] European Council (2008) On Ambient Air Quality and Cleaner Air for Europe 2008/50/EC, Off. J. Eur. Union, 1, 1–44, https://eur-lex.europa.eu/legal-content/EN/TXT/PDF/?uri=CELEX:32008L0050&from=en

[7] WHO. (2021). WHO global air quality guidelines. Particulate matter (PM2.5 and PM10), ozone, nitrogen dioxide, sulfur dioxide and carbon monoxide. Geneva: World Health Organization; 2021. Licence: CC BYNCSA 3.0 IGO.

[8] European Council (2024) Directive (EU) 2024/2881 of the European Parliament and of the Council of 23 October 2024 on ambient air quality and cleaner air for Europe (recast), Off. J. Eur. Union, 1–70, https://eur-lex.europa.eu/eli/dir/2024/2881

NO_2	$\mu g/m^3$	1 day	-	50	50
NO_2	$\mu g/m^3$	1 hour	200	200	200
$PM_{2.5}$	$\mu g/m^3$	1 year	25	10	5
SO_2	$\mu g/m^3$	1 year	-	20	-
SO_2	$\mu g/m^3$	1 day	125	50	40
SO_2	$\mu g/m^3$	1 hour	350	350	-

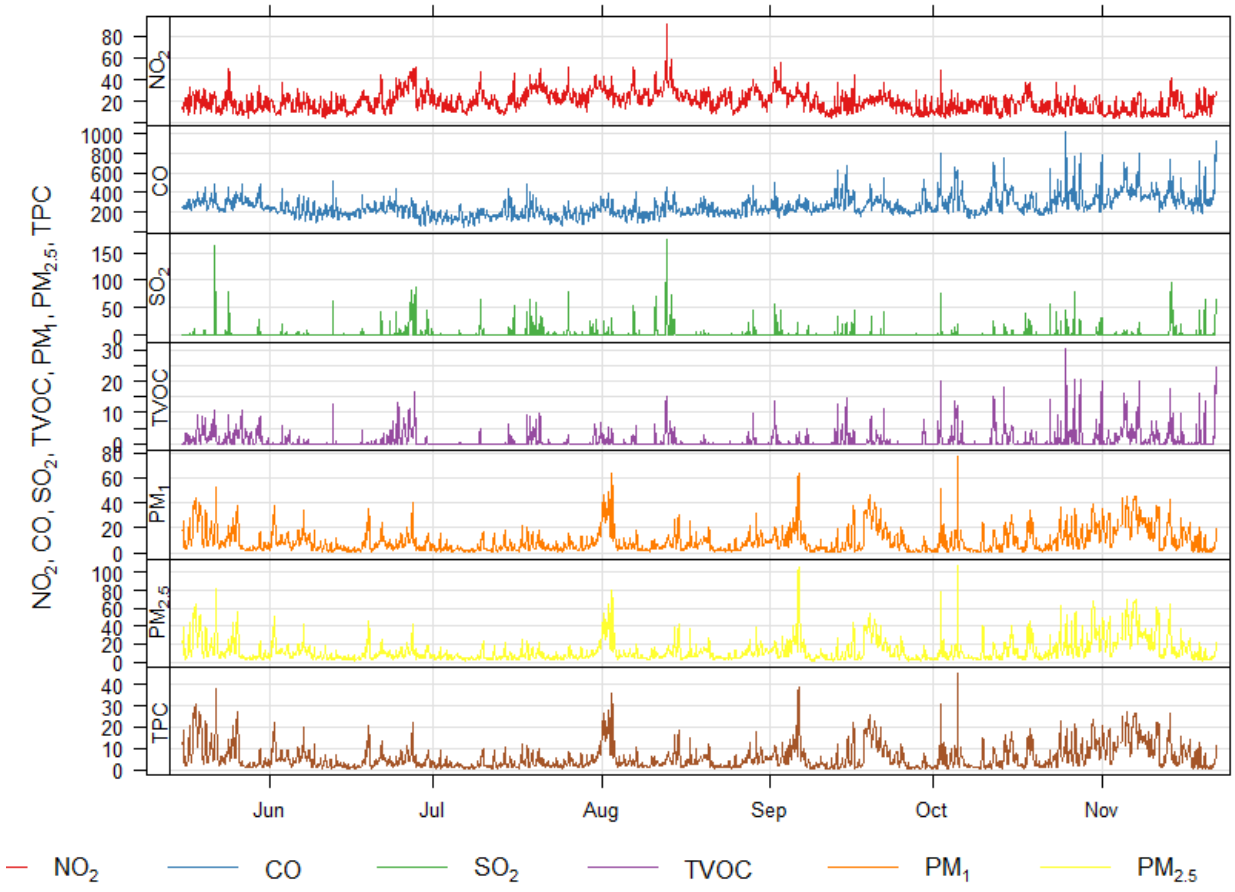

Figure 2. Observed hourly concentrations of all measured species between 16 May - 21 November 2024. All concentrations are reported in $\mu g/m^3$, except Total Particle Count (TPC) which is reported in count/m^3 and Total Volatile Compounds (TVOC) which is reported in ppb.

Meteorological analysis

Analysis of air pollutant concentrations recorded when different wind conditions occurred can give an indication about the locations of emission sources relative to a monitoring station. For example, where high NO_2 concentrations routinely coincide with the direction of the wind coming from the west, this can indicate that an emission source is located to the west of the monitoring location.

Relative to the location of the AQMesh monitor, Antwerp Airport is located to the east (terminal, main apron and runway), northeast (runway and peripheral buildings) and southeast (terminal, hangars and car park). The majority of Antwerp's built up area is to the northwest, north and west of the monitoring location, although there are built-up areas and major roads in all directions. Data from the European Industrial Emissions Portal for 2022[9] indicates that 5 km to the northwest there is a large cluster of industrial facilities that report emissions of VOCs, SO_2, NO_2 and other air pollutants.

During the monitoring period wind blew from all wind-sectors, but were most frequent from the southwest (Figure 3). Emission sources to the southwest may, therefore, make a larger contribution to the air pollution burden at the monitoring location even if the highest observed concentrations are linked with other wind directions. The frequency of winds from each direction is combined with pollutant observations in bottom panels of figures 4-10 to assess this contribution.

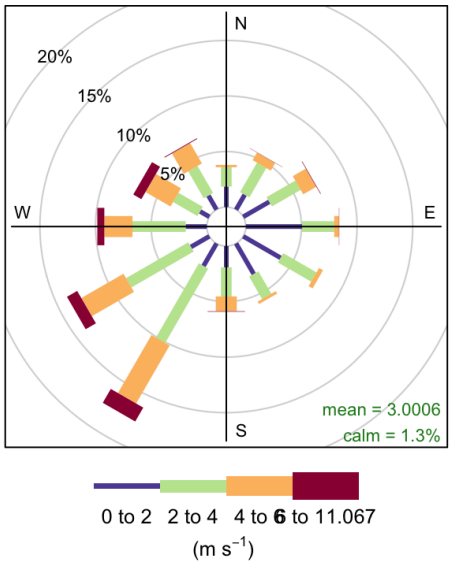

Frequency of counts by wind direction (%)

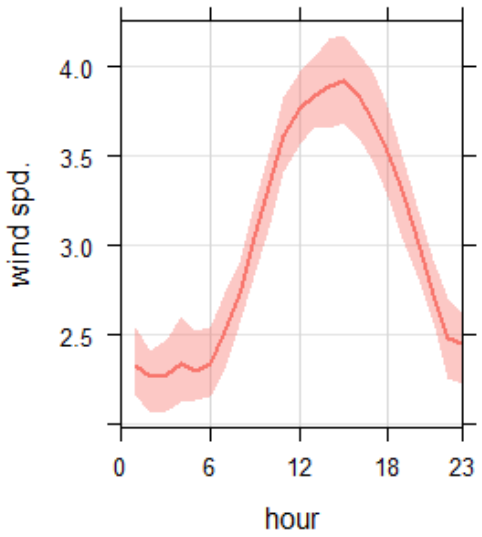

[9] European Environment Agency (2024). European Industrial Emissions Portal. https://industry.eea.europa.eu/explore/explore-data-map/map [Accessed 17/12/2024]

Figure 3. Wind data from 16 May - 21st November 2024 at Antwerp Airport. Left: Frequency of wind direction and speed Right: Average wind speed by hour of the day and 95% confidence interval.

The highest NO_2 concentrations during the monitoring period occurred when winds blew from the north and northwest. Concentrations were highest between 2200 and 2300 hours and during the mid-morning. Southwesterly winds made the greatest contribution to the NO_2 burden at the monitoring location due to the frequency of winds from this direction (Figure 4).

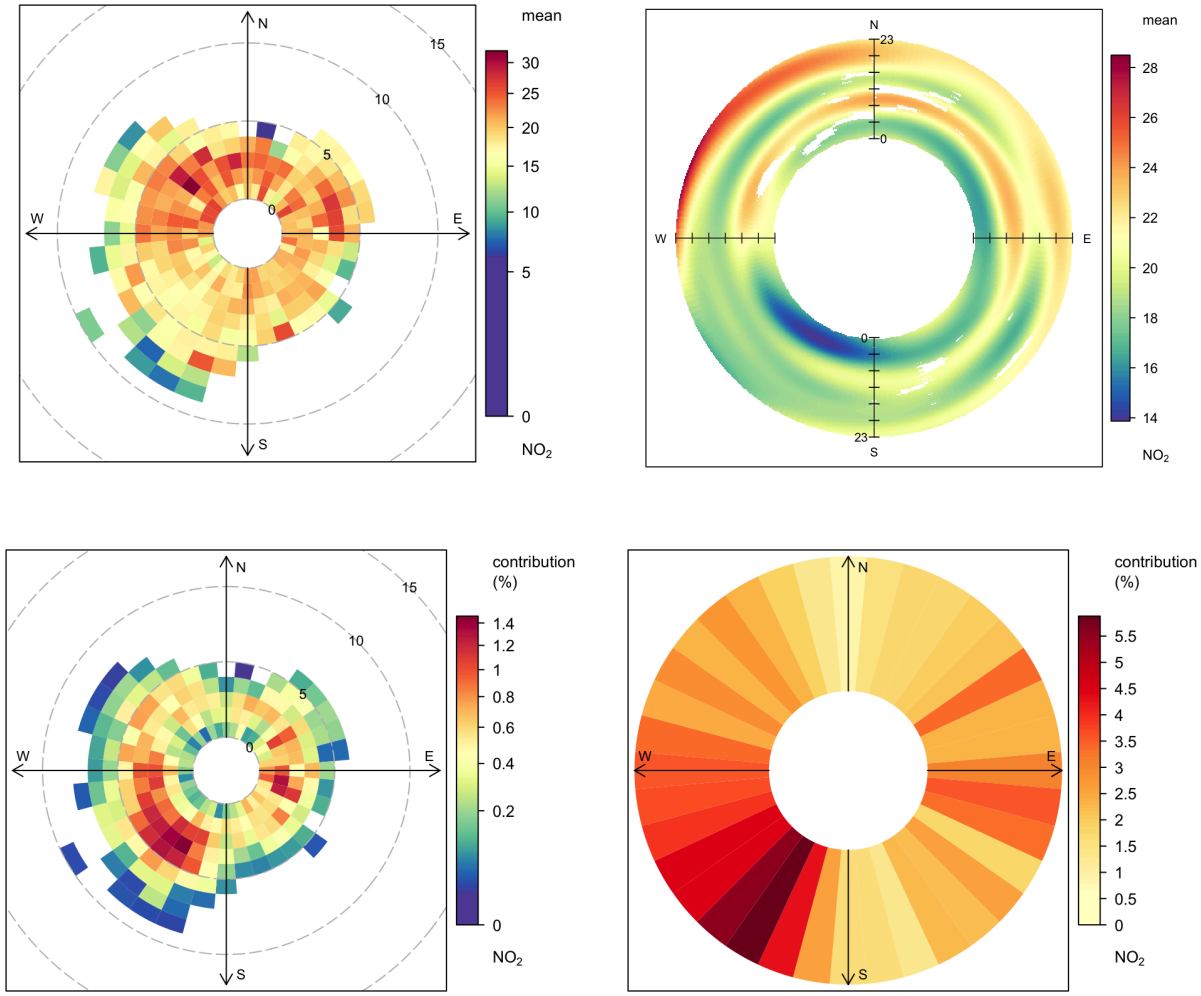

Figure 4. Observed NO_2 concentrations (µg/m³) at the monitoring site from 16 May - 21 November 2024 in relation to wind, time and frequency data. Top left: Concentration in relation to wind speed (m/s) and direction. Top right: Concentration in relation to

wind direction and time-of-day[10]. Bottom left: Contribution of wind speed and wind direction pairs to the pollutant burden at the monitoring location. Bottom right: Contribution of wind direction sectors to the pollutant burden at the monitoring location.

The highest CO concentrations during the monitoring period occurred when winds blew from the east and between late evening and late morning. CO concentrations were high during periods of low wind speed from all wind directions, indicating local sources such as road traffic and airport operations in the case of easterly winds. Higher night-time concentrations may be the result of a reduced boundary layer height, reduced atmospheric turbulence at night and higher wind speeds during the day. Southwesterly winds made the greatest contribution to the CO burden at the monitoring location due to the frequency of winds from this direction. Despite easterly winds being less frequent this wind sector also made a large contribution to the total CO burden observed (Figure 5).

[10] Colour shading indicates diurnal changes from the centre to the outer edge. The inside of the circle indicates average concentrations at 00:00 hours, the outer edge represents 23:00 hours.

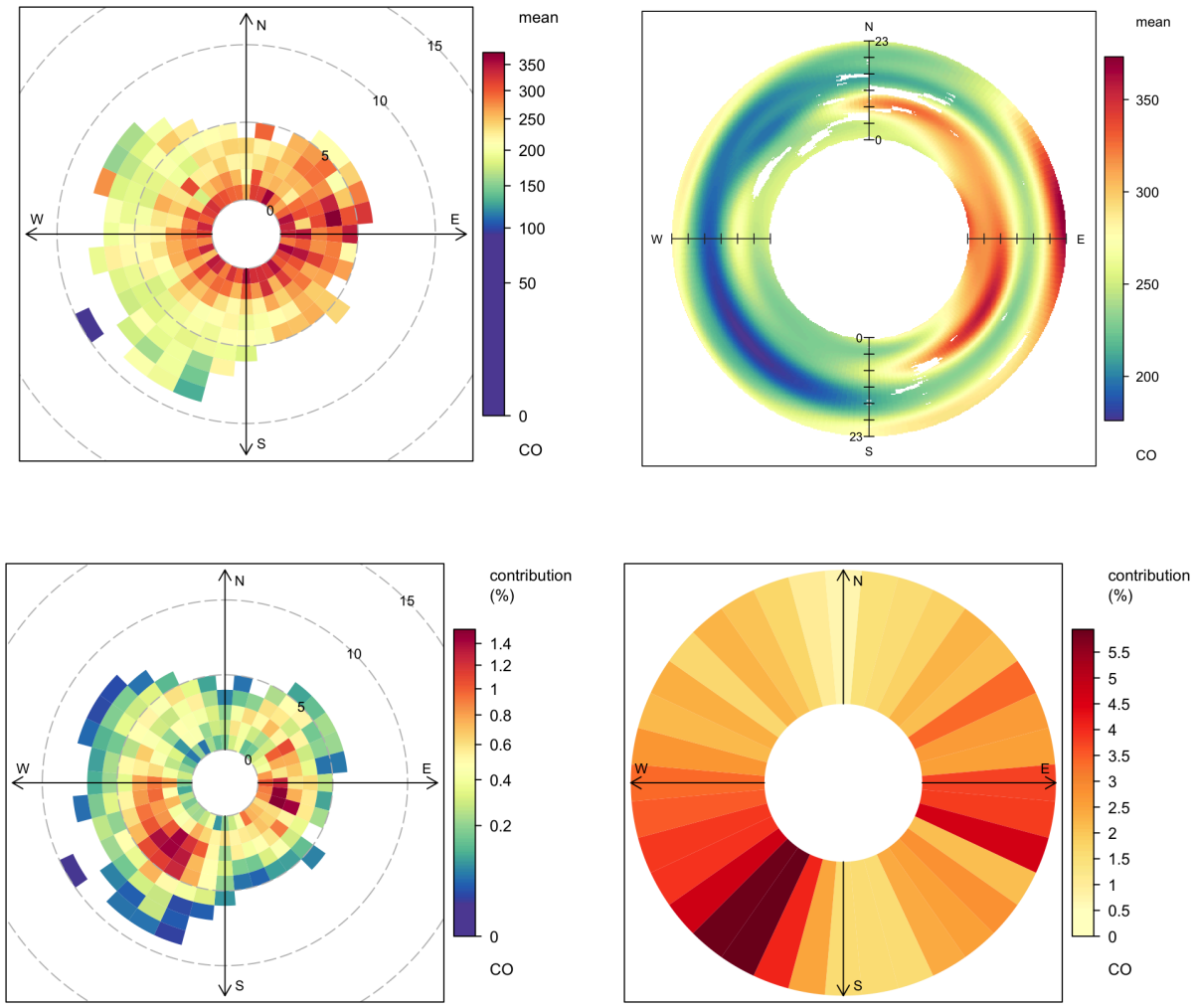

Figure 5. Observed CO concentrations (µg/m³) at the monitoring site from 16 May - 21 November 2024 in relation to wind, time and frequency data. Top left: Concentration in relation to wind speed (m/s) and direction. Top right: Concentration in relation to wind direction and time-of-day. Bottom left: Contribution of wind speed and wind direction pairs to the pollutant burden at the monitoring location. Bottom right: Contribution of wind direction sectors to the pollutant burden at the monitoring location.

The highest SO_2 concentrations during the monitoring period occurred when winds blew from the northwest and between 2200 and 2300 hours. The wind directions that made the greatest contribution to the SO_2 burden at the monitoring location were westerly and northwesterly winds, due to the frequency of winds from this direction and the higher concentration measured in each observation at these times (Figure 6).

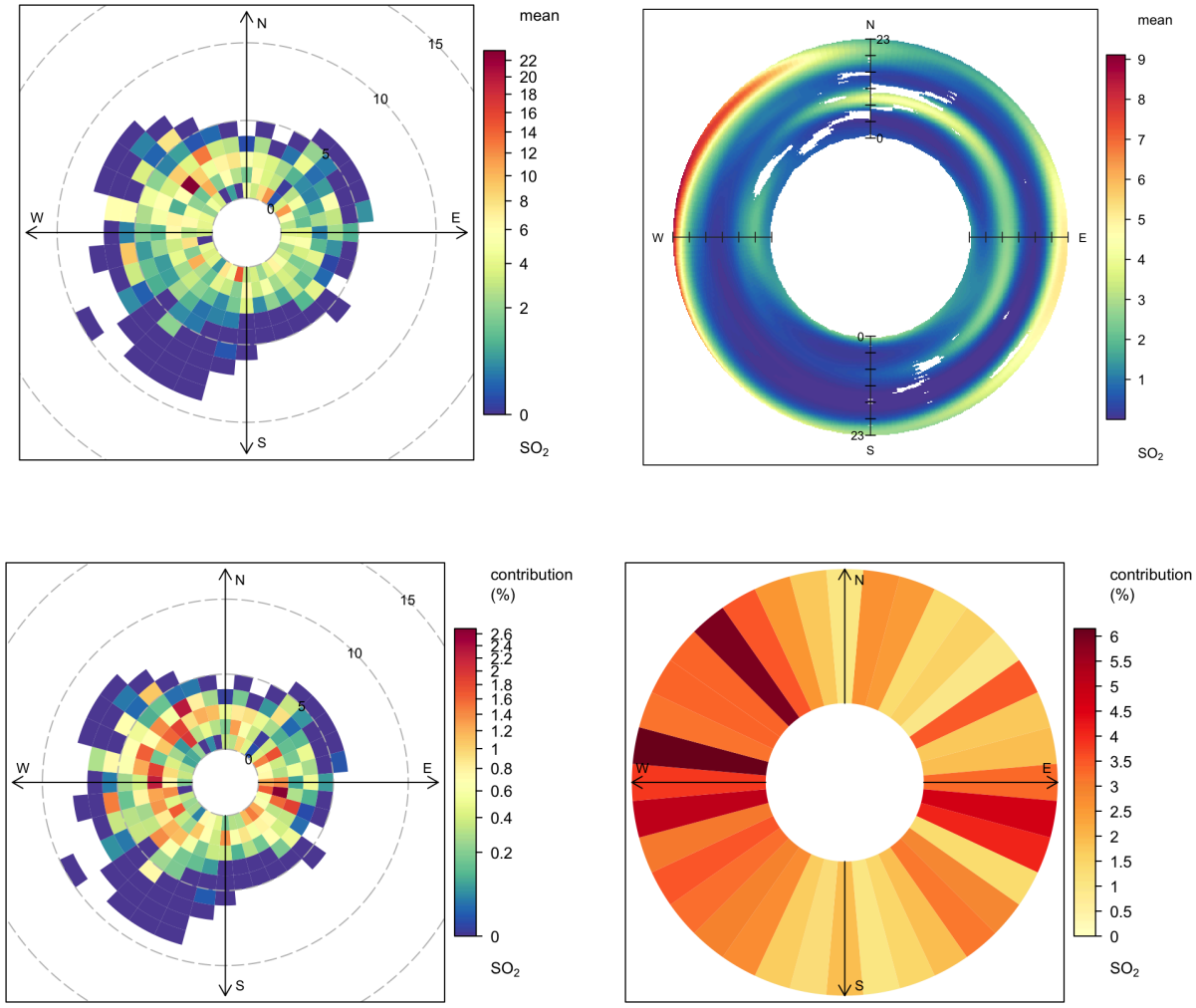

Figure 6. Observed SO_2 concentrations (µg/m³) at the monitoring site from 16 May - 21 November 2024 in relation to wind, time and frequency data. Top left: Concentration in relation to wind speed (m/s) and direction. Top right: Concentration in relation to wind direction and time-of-day. Bottom left: Contribution of wind speed and wind direction pairs to the pollutant burden at the monitoring location. Bottom right: Contribution of wind direction sectors to the pollutant burden at the monitoring location.

The highest particle counts during the monitoring period occurred when winds blew from the northeast and east. They were also highest during the first half of the day, lower concentrations during the afternoon coincide with higher wind speeds at that time. The wind directions that made the greatest contribution to the number of particles at the monitoring location were i) southwesterly winds, due to the frequency of winds from this direction, and ii) easterly winds, due to the high number of particles measured in each observation (Figure 7).

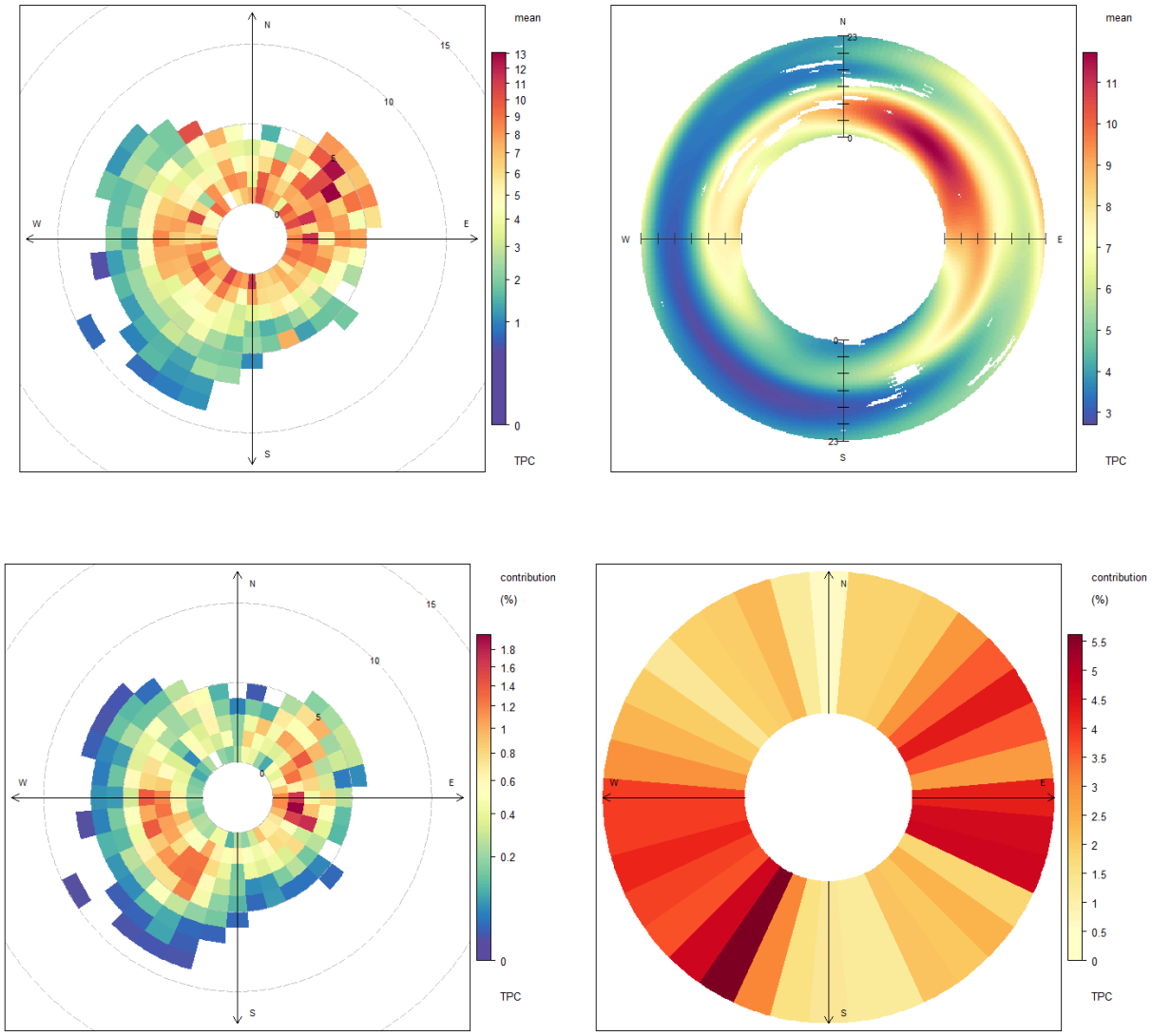

Figure 7. Observed total particle count (count/m³) at the monitoring site from 16 May - 21 November 2024 in relation to wind, time and frequency data. Top left: Concentration in relation to wind speed (m/s) and direction. Top right: Concentration in relation to wind direction and time-of-day. Bottom left: Contribution of wind speed and wind direction pairs to the pollutant burden at the monitoring location. Bottom right: Contribution of wind direction sectors to the pollutant burden at the monitoring location.

The highest PM_1 concentrations during the monitoring period occurred when winds blew from the northeast and during the first half of the day. The wind directions that made the greatest contribution to the PM_1 burden at the monitoring location were i) southwesterly winds, due to the frequency of winds from this direction, and ii)

northeasterly-southeasterly winds, due to the high PM_1 concentration measured in each observation. Despite easterly winds being less frequent this wind sector also made a large contribution to the total PM_1 burden observed (Figure 8).

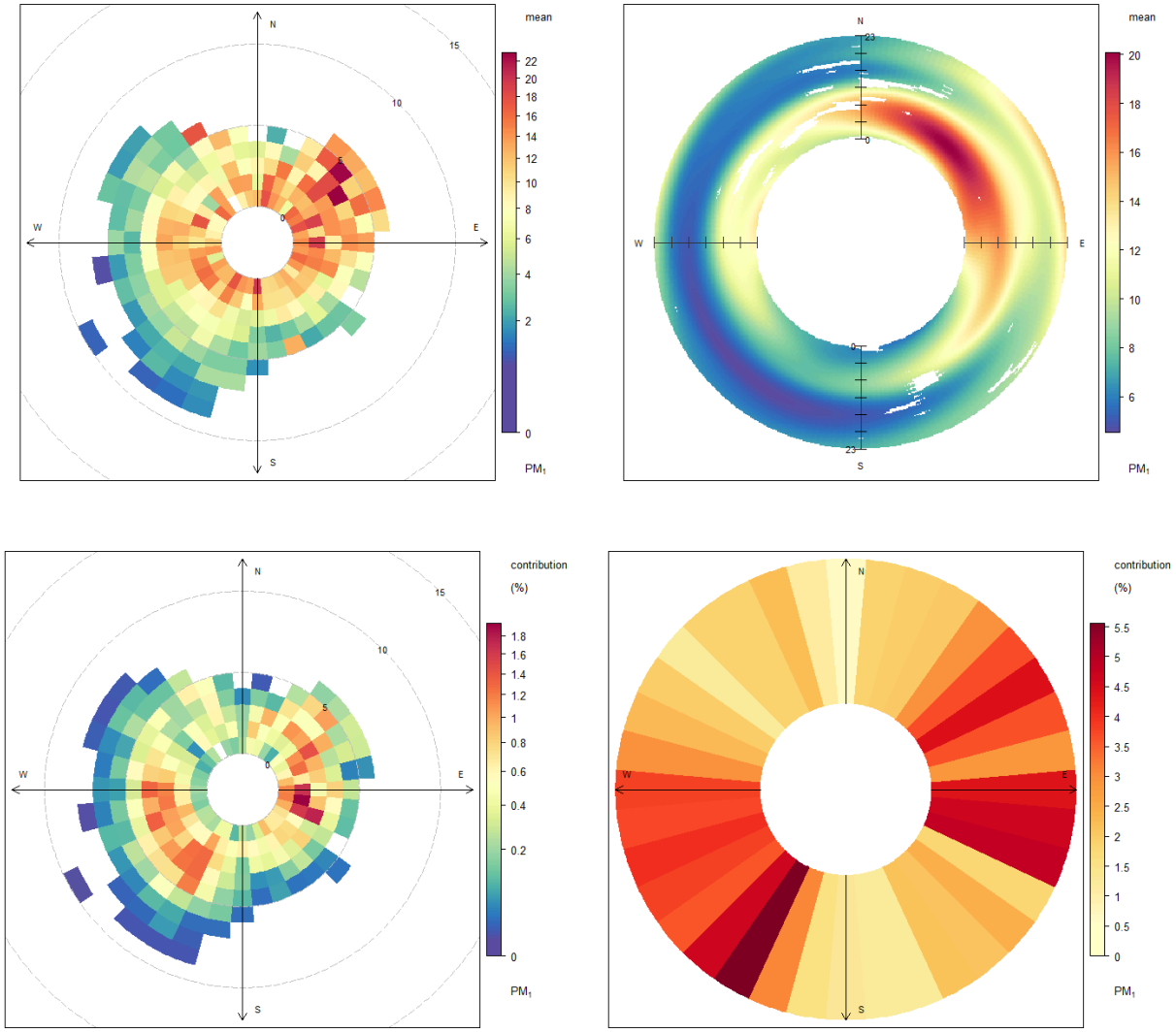

Figure 8. Observed PM_1 concentrations (µg/m³) at the monitoring site from 16 May - 21 November 2024 in relation to wind, time and frequency data. Top left: Concentration in relation to wind speed (m/s) and direction. Top right: Concentration in relation to wind direction and time-of-day. Bottom left: Contribution of wind speed and wind direction pairs to the pollutant burden at the monitoring location. Bottom right: Contribution of wind direction sectors to the pollutant burden at the monitoring location.

The highest $PM_{2.5}$ concentrations during the monitoring period occurred when winds blew from the northeast and during the first half of the day. The wind directions that made the greatest contribution to the $PM_{2.5}$ burden at the monitoring location were i) southwesterly winds, due to the frequency of winds from this direction, and ii) northeasterly-easterly winds, due to the high $PM_{2.5}$ concentration measured in each observation (Figure 9). Overall, the observations of TPC, PM_1 and $PM_{2.5}$, are closely correlated, suggesting common influences on the dynamics of these species.

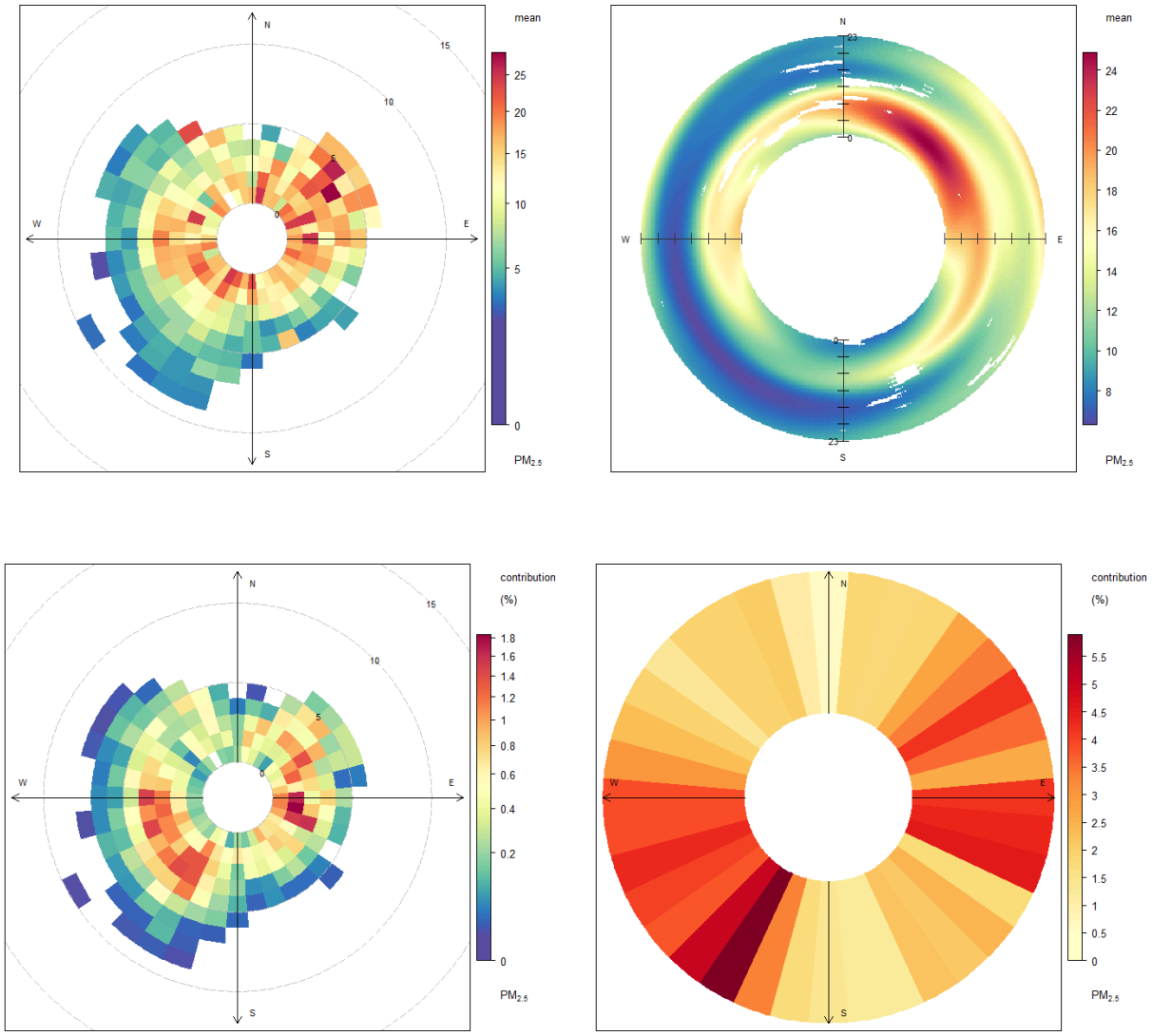

Figure 9. Observed $PM_{2.5}$ concentrations (µg/m³) at the monitoring site from 16 May - 21 November 2024 in relation to wind, time and frequency data. Top left: Concentration in relation to wind speed (m/s) and direction. Top right: Concentration

in relation to wind direction and time-of-day. Bottom left: Contribution of wind speed and wind direction pairs to the pollutant burden at the monitoring location. Bottom right: Contribution of wind direction sectors to the pollutant burden at the monitoring location.

The highest TVOC concentrations during the monitoring period occurred when winds blew from the east and during the late morning and late evening (Figure 10). Easterly winds also made the greatest contribution to the TVOC burden at the monitoring location, due to the high TVOC concentration measured in each observation despite this not being the predominant wind direction.

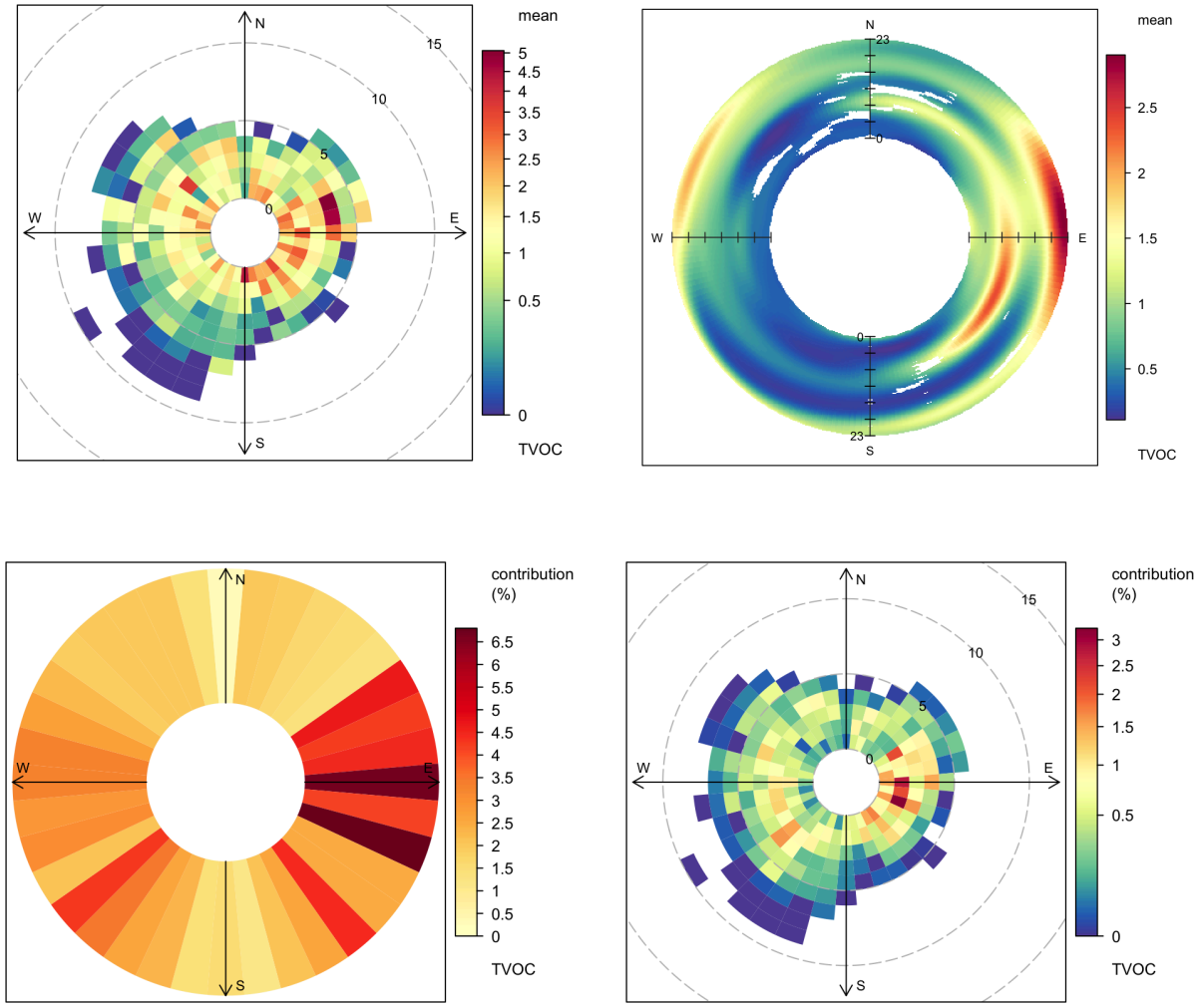

Figure 10. Observed TVOC concentrations (ppb) at the monitoring site from 16 May - 21 November 2024 in relation to wind, time and frequency data. Top left: Concentration in relation to wind speed (m/s) and direction. Top right: Concentration in relation to wind direction and time-of-day. Bottom left: Contribution of wind speed and wind

direction pairs to the pollutant burden at the monitoring location. Bottom right: Contribution of wind direction sectors to the pollutant burden at the monitoring location.

When split according to wind direction, average concentrations of PM_1, $PM_{2.5}$, and TVOCs during the monitoring period were highest when winds blew from the east and northeast. This is the direction of Antwerp Airport. The same pattern was observed for total particle count (Figure 11). Average NO_2 and SO_2 concentrations were highest during northwesterly winds. This coincides with the centre of Antwerp and the industrial area 5 km to the northwest. Average CO concentrations were highest during easterly winds. This is the direction of Antwerp Airport. The relatively short lifetime of CO means that concentrations are often determined by nearby emissions which could include road traffic or airport activity in this case.

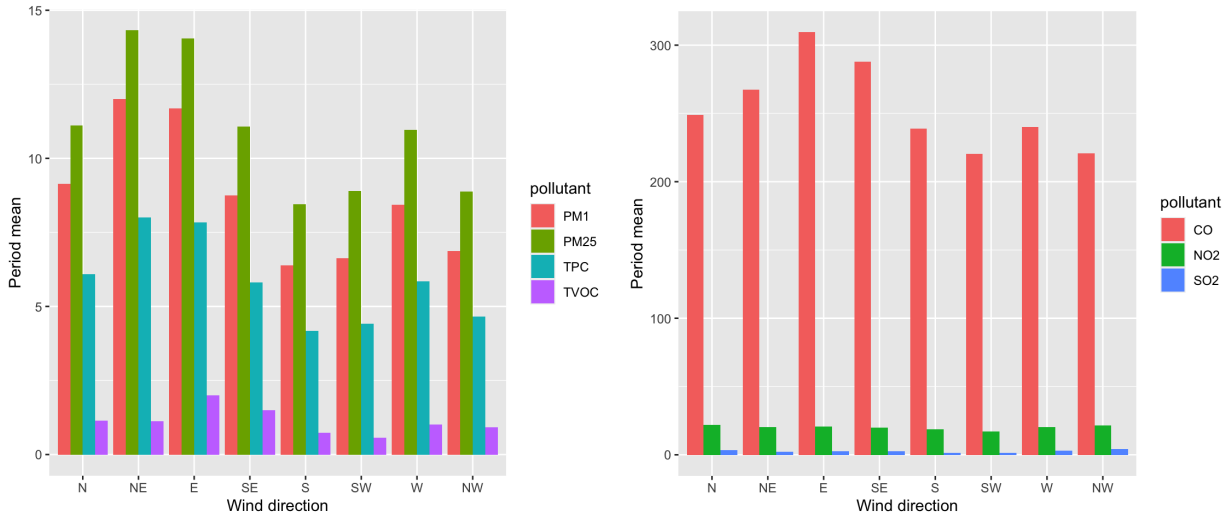

Figure 11. Monitoring period mean observed pollutant concentrations by wind direction (16 May - 21 November 2024). Left: Particulate mapper (PM_1, $PM_{2.5}$, total particle count) and total VOCs. Right: Combustion gases (CO, NO_2, SO_2). All concentrations are reported in $\mu g/m^3$, except Total Particle Count (TPC) which is reported in count/m^3 and Total Volatile Compounds (TVOC) which is reported in ppb.

Conclusion

Observations of PM_1, $PM_{2.5}$, TPC, TVOC, NO_2, CO and SO_2 were made at a residential location close to Antwerp airport. Average observed concentrations were within current European Union standards and World Health Organisation guidelines for air quality over comparable averaging periods. Minimum and maximum hourly concentrations indicate significant variability. Variability associated with wind

direction, wind speed and time of day was used to investigate possible local air pollution sources.

Higher NO_2 and SO_2 observations were associated with winds from the northwest. Sources of NO_2 and SO_2 in this direction include Antwerp city centre and the industrial area to the north-west of Antwerp.

Of the other pollutants measured (CO, VOCs and fine particulate matter), there were observations suggesting that sources to the east were important contributors to the pollution burden at the monitoring location. This wind direction coincides with the location of Antwerp Airport.

Easterly winds were associated with high particle counts and a large contribution to the number of particles observed at the monitoring station. Easterly winds were associated with high fine particulate matter (PM_1, $PM_{2.5}$) concentrations, and a large contribution to the burden of fine particulate matter pollution at the monitoring station. Easterly winds were associated with high TVOC concentrations, and a large contribution to the burden of TVOC pollution at the monitoring station. However the timing of the highest TVOC observations differed to the timing of the highest fine particulate matter observations.

Appendix 1. AQMesh cross-comparison

The AQMesh air quality monitoring instrument uses electrochemical sensors to determine ambient concentrations of trace gases. The sensors are sensitive to the environment, including the effects of temperature and humidity. Raw data gathered by the electrochemical gas sensors is processed by a proprietary algorithm which corrects for these effects using temperature, relative humidity and atmospheric pressure measurements also made by the AQMesh monitor.

A local field-calibration was conducted by colocating the AQMesh with the Antwerp Borgerhout monitoring station (42R801) by arrangement with the Flanders Environment Agency. The colocation allowed comparison with a reference quality instrument to determine scaling factors which were then applied to the AQMesh NO and NO_2 measurements. The Borgerhout monitoring station is located close to the junction of the N184 and Montensstraat on the eastern side of Antwerp city centre. It reports hourly concentrations of $PM_{2.5}$, PM_{10}, NO and NO_2.

The AQMesh pod was co-located with the reference monitor between 29th of March 2024 and 6th of May 2024 (Figure A1).

Pre-calibration results from the co-location are shown in Figures A1 and A4 for NO and NO_2. The relationship between the AQMesh and reference monitor results is shown in Figures A2

and A5 which indicates that the AQMesh monitor differed from the reference monitor for NO (R^2=0.22) but was in good agreement for NO2 (R^2=0.64).

Pre-calibration results from the co-location are shown in Figures A7 and A10 for PM_1 and $PM_{2.5}$. The relationship between the AQMesh and reference monitor results is shown in Figures A8 and A11 which indicates that the AQMesh monitor was in good agreement for PM_1 (R^2=0.91) and $PM_{2.5}$ (R^2=0.89).

The scaling factors shown in Table A1 were then applied to the AQMesh monitoring results to improve the performance of the instrument during its deployment. The scaled results of the field-calibration are shown in Figures A3, A6, A9 and A12 for NO, NO_2, PM_1 and $PM_{2.5}$ respectively.

Table A1: Comparison of AQMesh and reference monitor data

	NO	NO_2	PM_1	$PM_{2.5}$
Slope	0.32	0.65	1.21	1.25
Intercept	1.43	2.66	-0.69	-0.91
Units	ppb	ppb	$\mu g/m^3$	$\mu g/m^3$

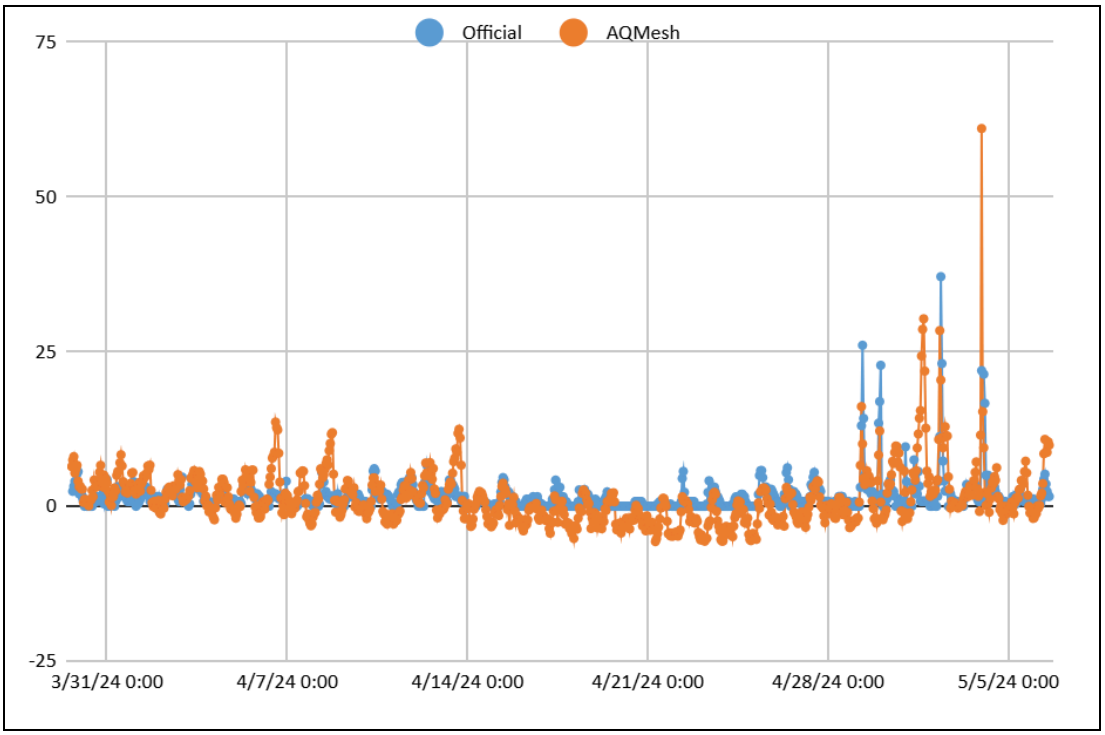

Figure A1: Measured NO concentration (ppb) from AQMesh (pre-calibration) and reference monitor

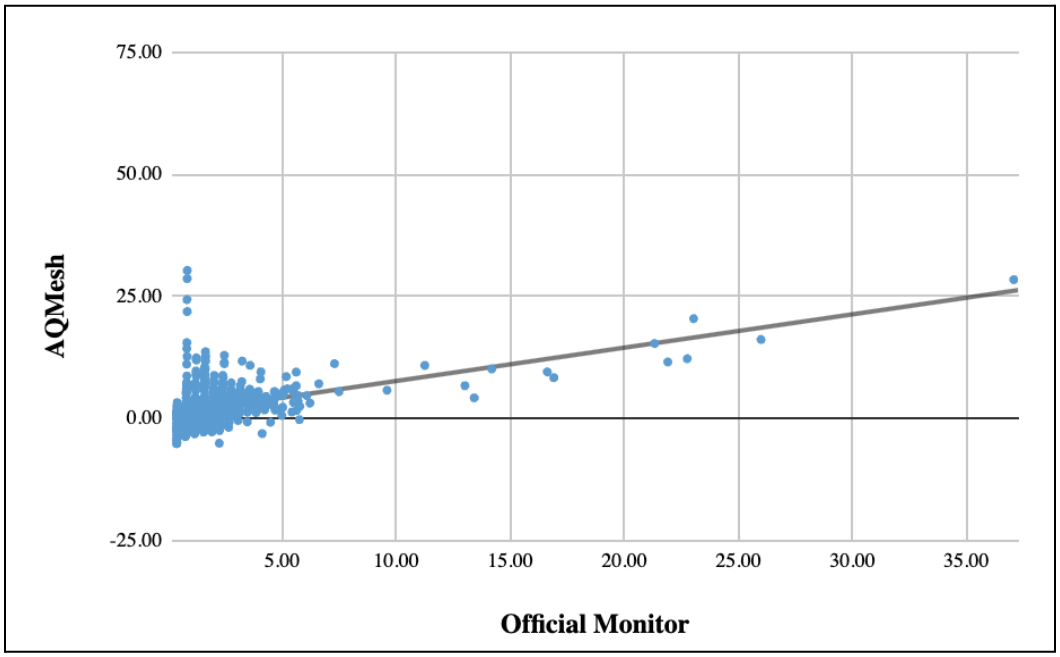

Figure A2: Comparison of AQMesh and reference monitor measured NO concentration (ppb)

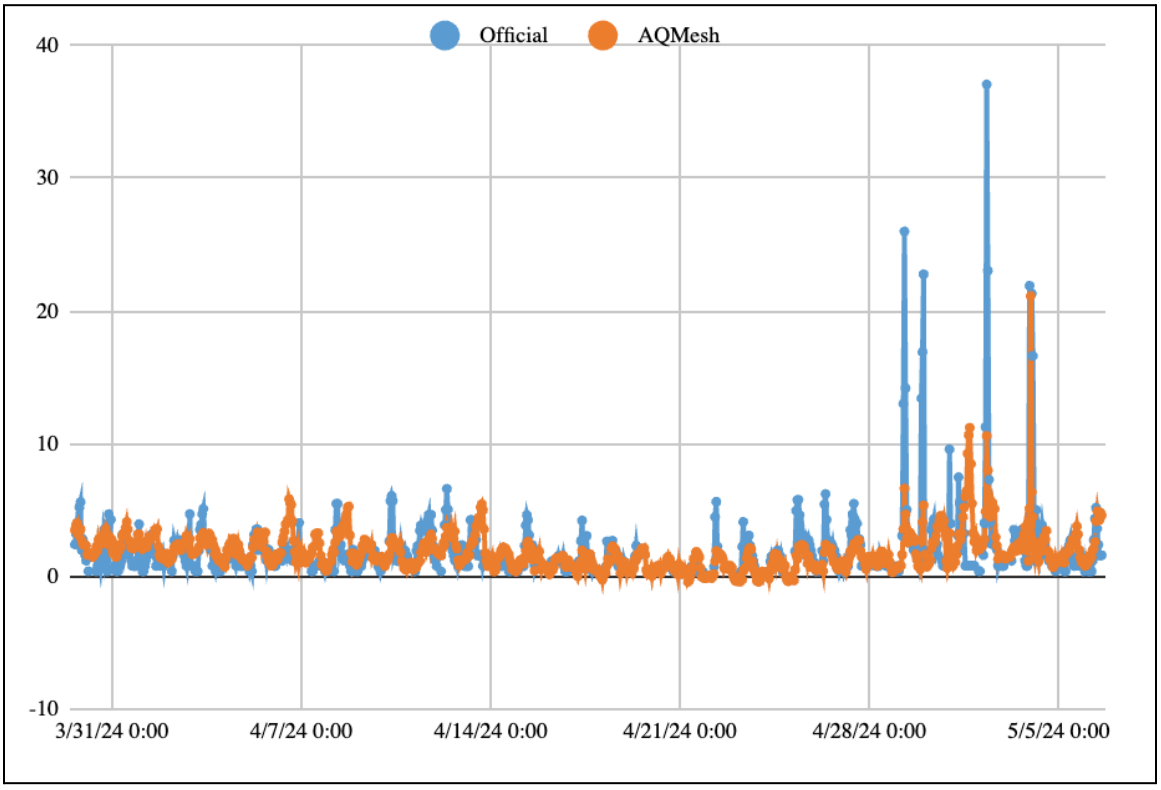

Figure A3: Measured NO concentration (ppb) from AQMesh (adjusted) and reference monitor

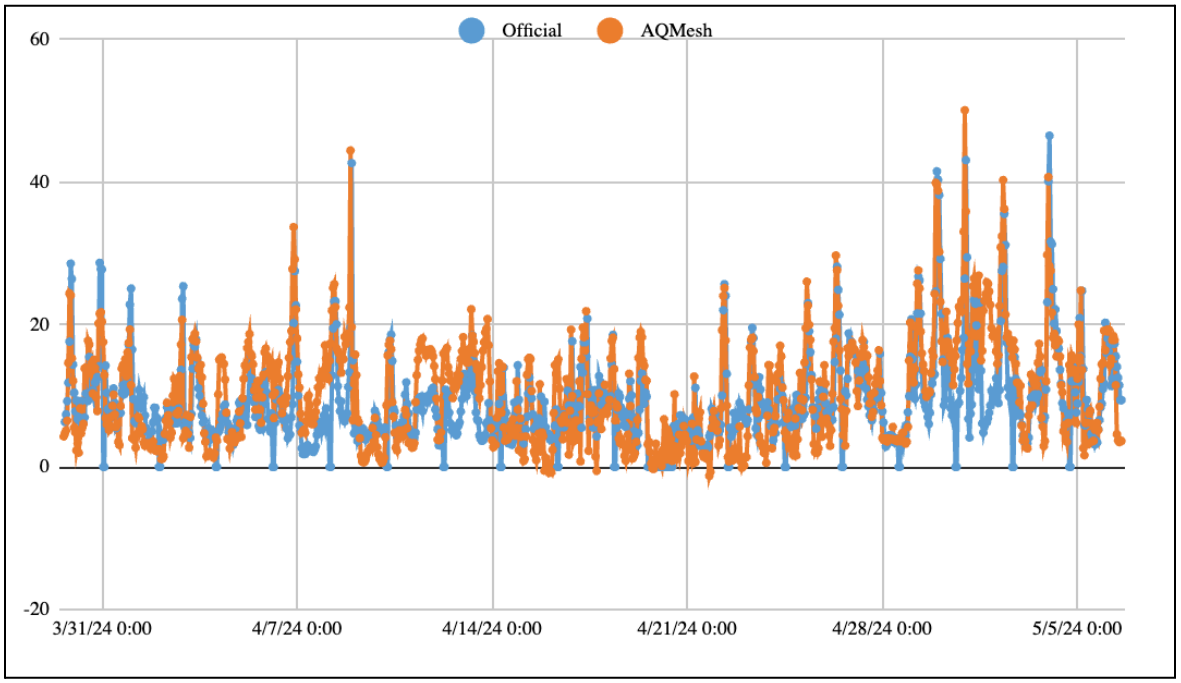

Figure A4: Measured NO_2 concentration (ppb) from AQMesh (pre-calibration) and reference monitor

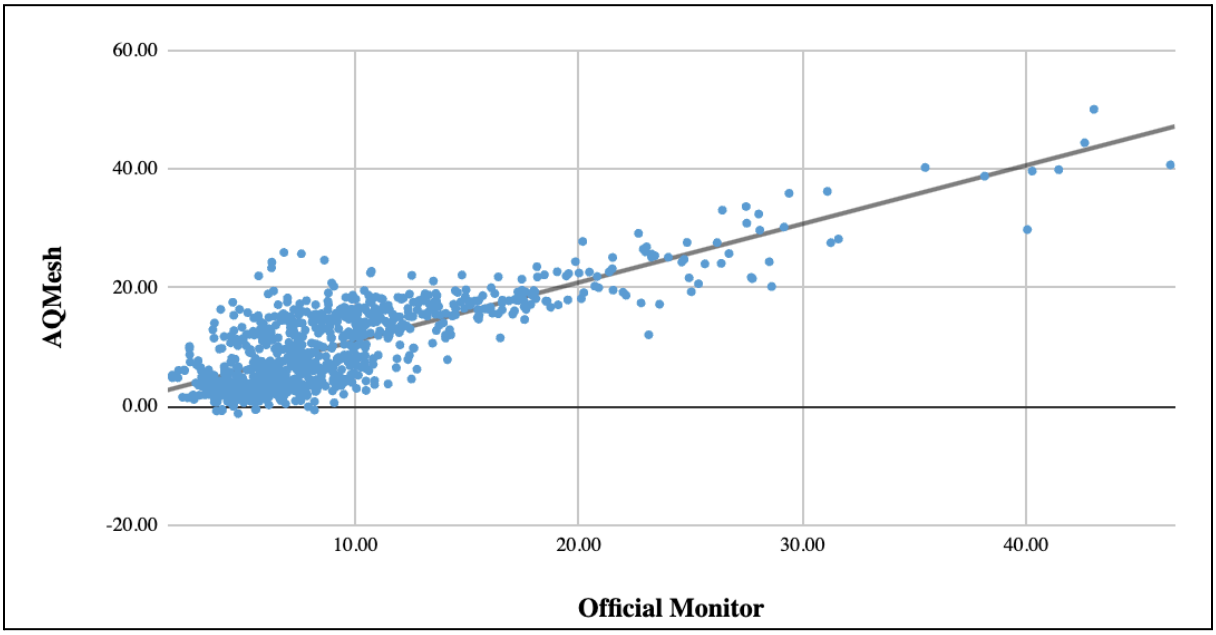

Figure A5: Comparison of AQMesh and reference monitor measured NO_2 concentration (ppb)

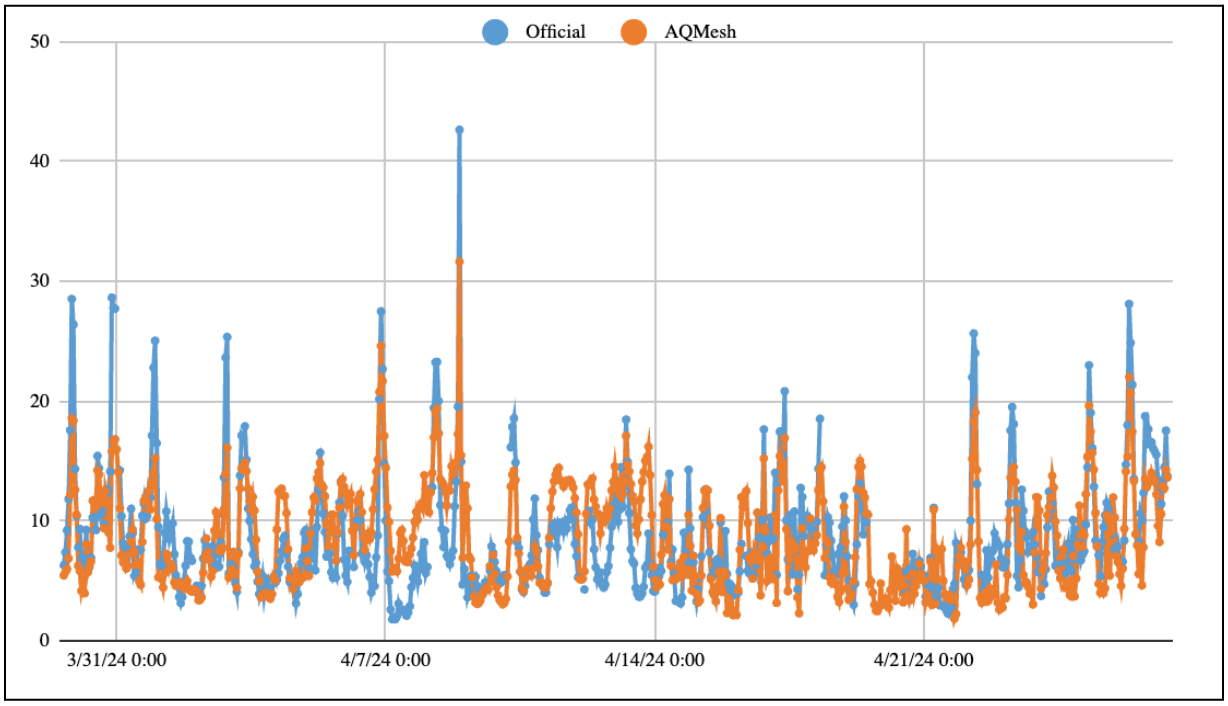

Figure A6: Measured NO_2 concentration (ppb) from AQMesh (adjusted) and reference monitor

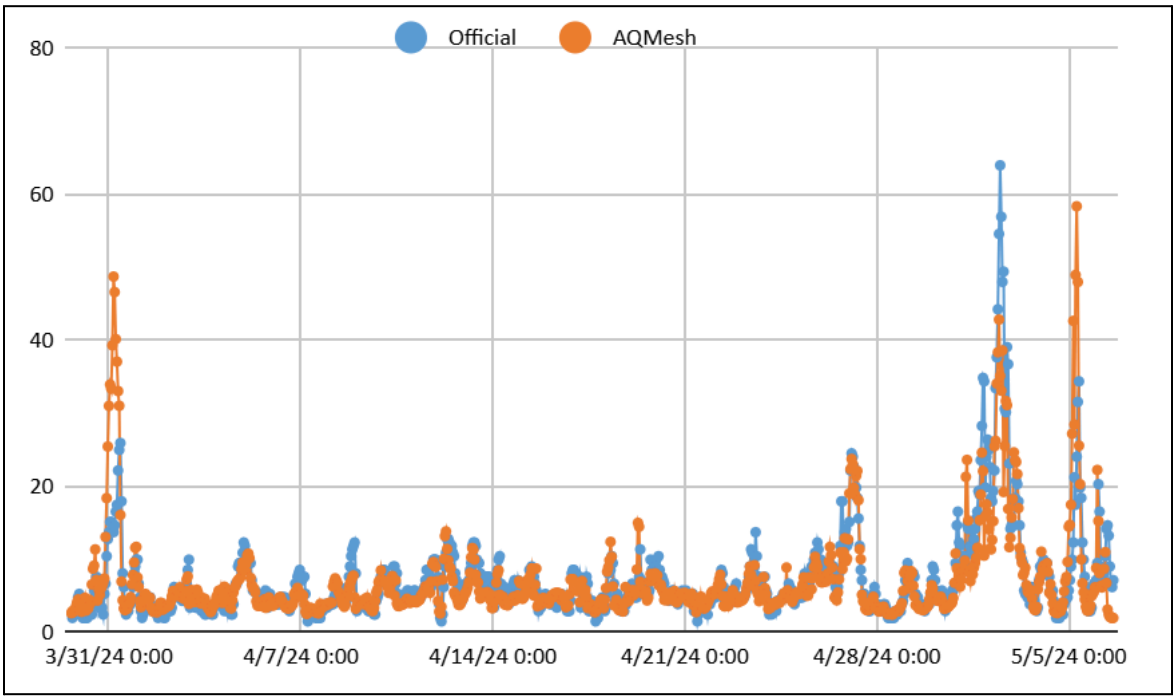

Figure A7: Measured PM_1 concentration ($\mu g/m^3$) from AQMesh (pre-calibration) and reference monitor

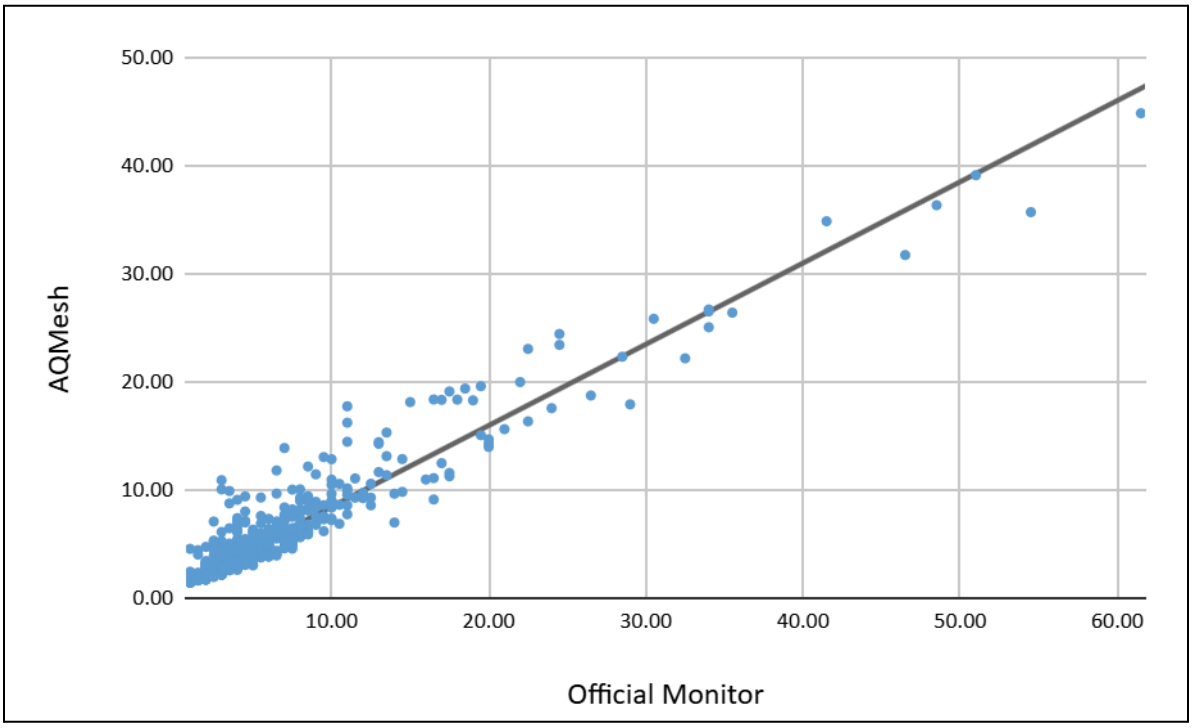

Figure A8: Comparison of AQMesh and reference monitor measured PM_1 concentration ($\mu g/m^3$)

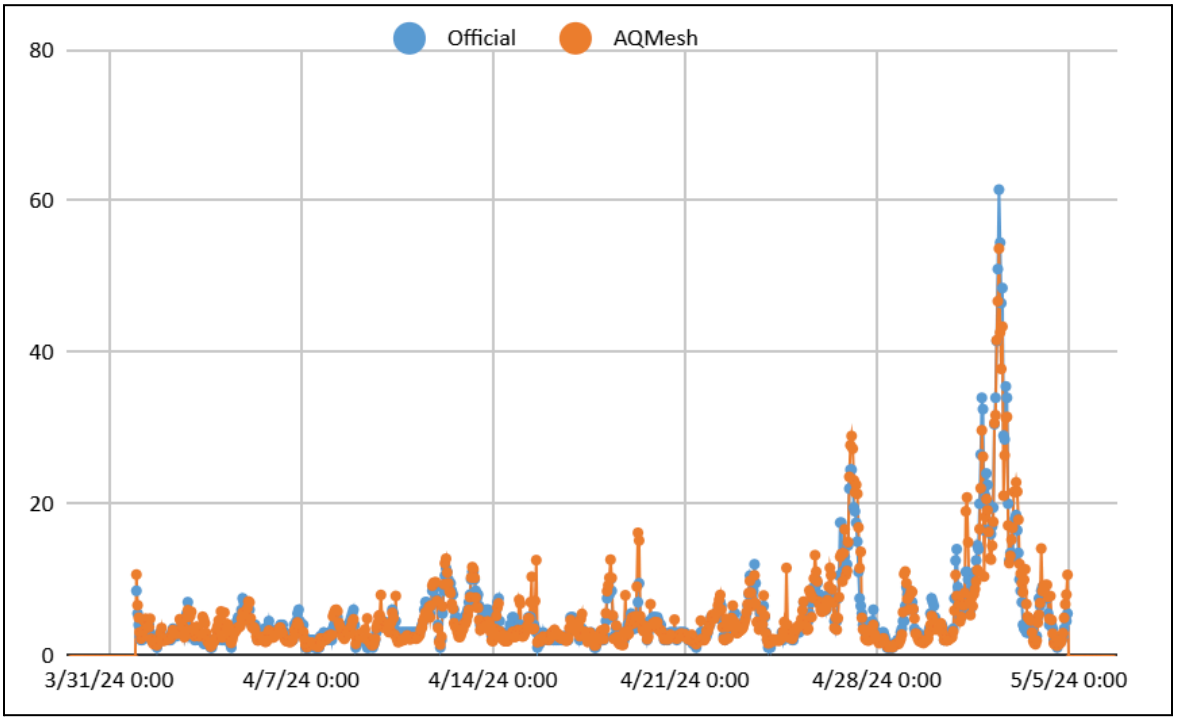

Figure A9: Measured PM_1 concentration ($\mu g/m^3$) from AQMesh (adjusted) and reference monitor

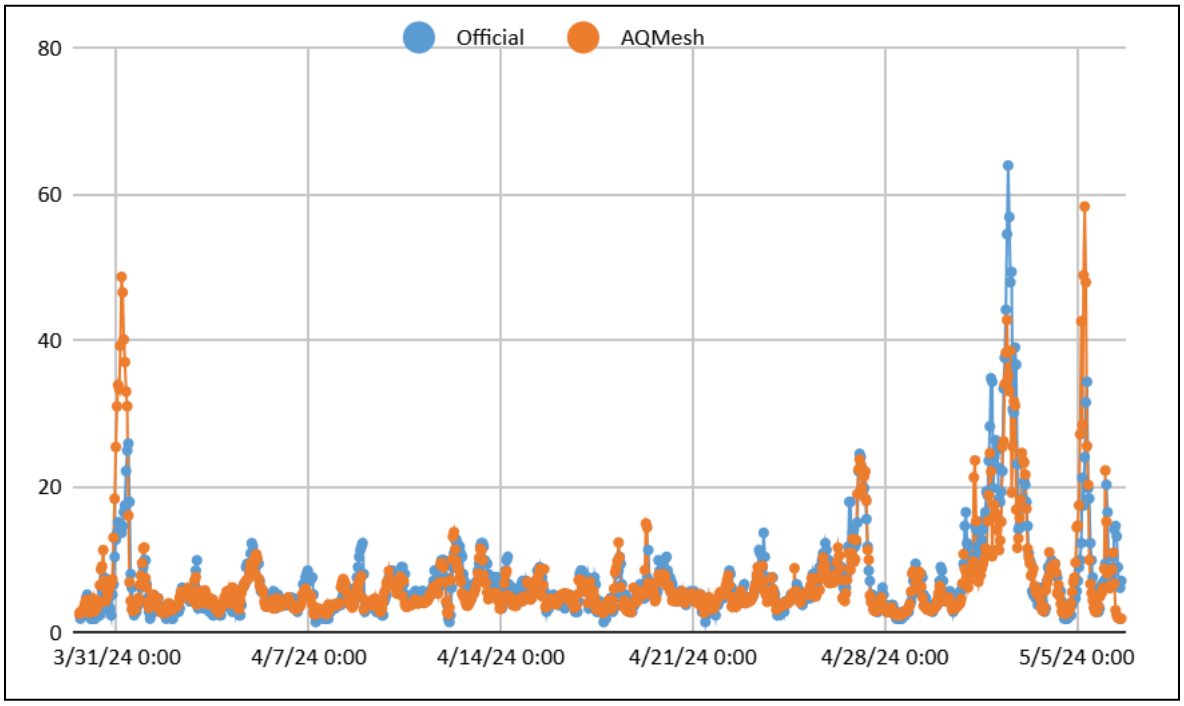

Figure A10: Measured $PM_{2.5}$ concentration ($\mu g/m^3$) from AQMesh (pre-calibration) and reference monitor

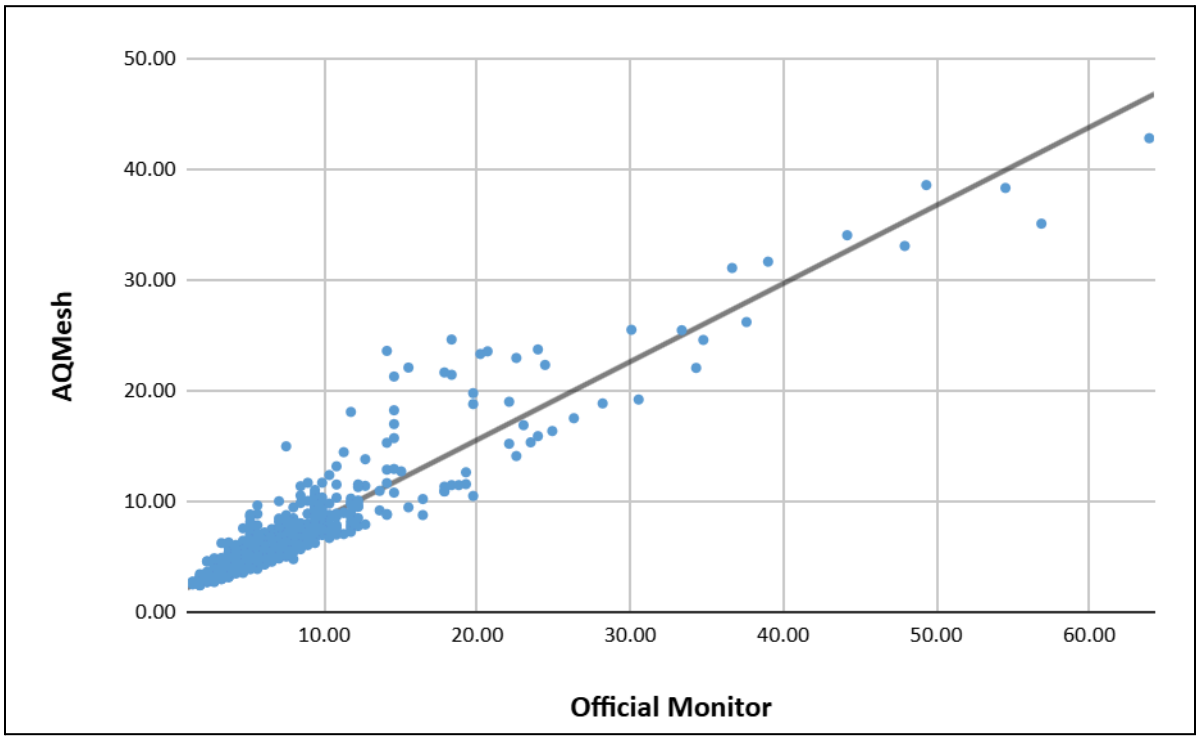

Figure A11: Comparison of AQMesh and reference monitor measured $PM_{2.5}$ concentration ($\mu g/m^3$)

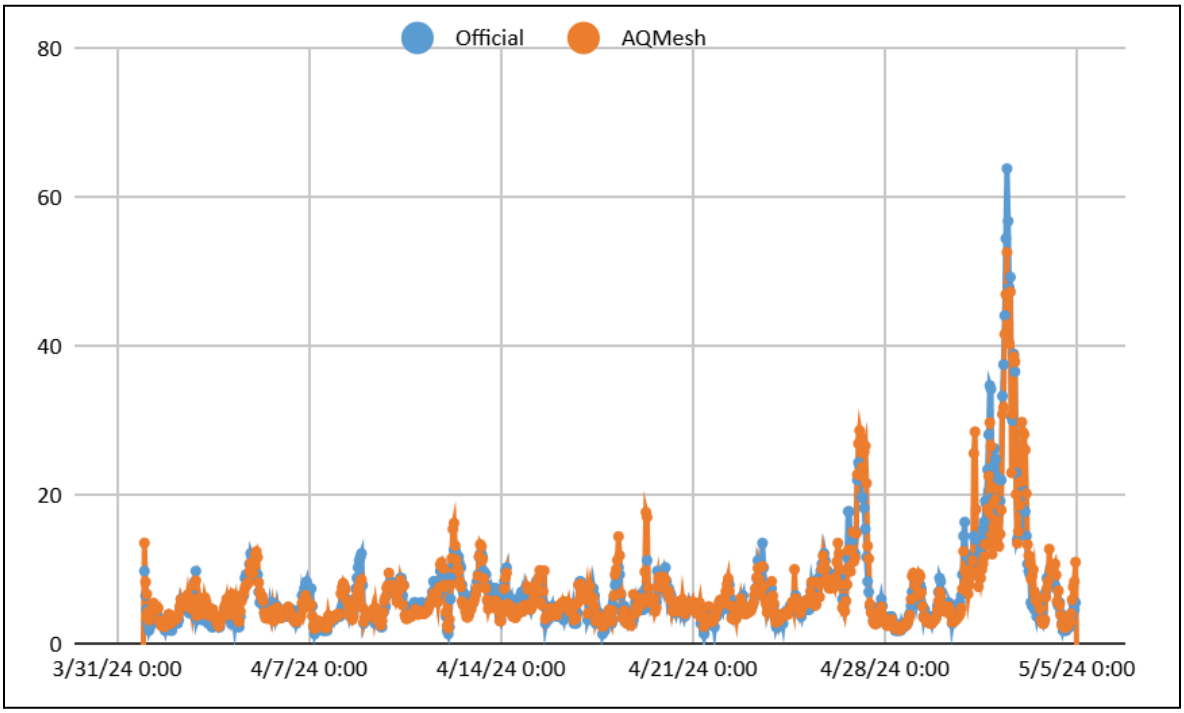

Figure A12: Measured $PM_{2.5}$ concentration ($\mu g/m^3$) from AQMesh (adjusted) and reference monitor